Supplement of Earth Syst. Sci. Data, 15, 1947–1968, 2023
https://doi.org/10.5194/essd-15-1947-2023-supplement

Open Access Earth System Science Data

Supplement of

Two years of volatile organic compound online in situ measurements at the Site Instrumental de Recherche par Télédétection Atmosphérique (Paris region, France) using proton-transfer-reaction mass spectrometry

Leïla Simon et al.

Correspondence to: Valérie Gros (valerie.gros@lsce.ipsl.fr)

Section 1: Supplementary text to the Instrumentation

Text S1: Kinetic approach for volume mixing ratio calculation using instrumental transmission

To obtain the sensitivity (in ncps/ppb) of compounds not present in the calibration standard, first the transmission of compounds present in the standard is calculated, based on the instrument's parameters and following Equation S1 (Taipale et al., 2008):

$$\frac{T_{RH^+}}{T_{H_3O^+}} = 10^9 \frac{p_{drift}}{I_{norm} p_{norm}} \frac{\mu_0 N_0}{kL} \frac{E}{N^2} S_{norm} \quad \text{(S1)}$$

With p_{drift} being the drift pressure, I_{norm} the normalized intensity (equal to 10^6), p_{norm} the normal pressure, μ_0 being the reduced ion mobility of the primary ions and equal to 2.8 $cm^2 \cdot V^{-1} \cdot s^{-1}$, N_0 the number density of air at standard conditions, k being the reaction rate constant of the given compound, L the length of the drift tube, $E=U_{drift}/L$, $N=N_A p_{drift}/(RT_{drift})$, and S_{norm} the normalized sensitivity obtained by a standard calibration. The k rates used in this study are summarized in Table 1; for unknown compounds or rates, a value of $3 \cdot 10^{-9} \cdot cm^3 \cdot s^{-1} \cdot molecule^{-1}$ is used, as usually recommended, because most proton transfer reaction constants range $2\text{-}4 \cdot 10^{-9} \cdot cm^3 \cdot s^{-1} \cdot molecule^{-1}$ (ACTRIS guidelines, Holzinger, 2015).

From the transmission coefficients of calibrated m/z, a transmission curve is modelled, from which the transmission coefficients of the other m/z are extracted and used to retrieve the sensitivity (S_{norm}) using a reversed equation of (S1).

Text S2: Discussion for tentative attribution of the measured m/z, based on PTR-ToF-MS measurements and the literature

m/z 31 was assigned to CH_2O (formaldehyde), which cannot be precisely quantified by PTR-MS, due to its proton affinity being too close to that of water, and is thus defined as its proxy. *m/z 33* was assigned to CH_3OH (methanol), the main alcohol present in the atmosphere, and is also the most important oxygenated VOC; although at this mass there are interferences from O_2^+, thus resulting in a high background. *At m/z 42,* CH_3CN (acetonitrile) is the main compound measured; interferences from other compounds are negligible (Yuan et al., 2017b). Acetaldehyde is the main component detected at *m/z 45* (de Gouw and Warneke, 2007). *m/z 46* can correspond to several compounds: it was mostly identified as CH_3NO and C_2H_7N, respectively formamide and dimethylamine, both compounds emitted by agricultural activities (Yuan et al., 2017a; Kammer et al., 2019). However, a few studies reported this mass as NO_2^+, that would correspond notably to peroxyacetyl nitrate (PAN) fragmentations (Yuan et al., 2017b) or other organic nitrates (Aoki et al., 2007; Duncianu et al., 2017), but cannot be precisely quantify using H_3O^+ ionization. In this study, we will refer to it as m/z 46 (or m46). *m/z 47* corresponds to C_2H_6O (ethanol) and CH_2O_2 (formic acid) and will therefore be referred to as their sum, although the sensitivity of ethanol is lower than that of formic acid. Their seasonal contribution can be found in Table 2, and shows that *m/z 47* is dominated by formic acid in spring and summer (> 90%), but in autumn and winter, ethanol contribution becomes significant. This is a similar trend to that of furan's and isoprene's contributions to m/z 69. *m/z 57* is usually attributed to propenal (C_3H_4O) (Knighton et al., 2007;

Languille et al., 2020), but there are interferences from C_4H_8: butenes or other hydrocarbons' fragmentations, that cannot be precisely quantified but seem to be dominant in our study (Table 2). *m/z 58* was assigned to allylamine, a compound emitted by agricultural activities (Kammer et al., 2019). *m/z 59* could be correspond to C_3H_6O (acetone + propanal), C_4H_{10} (butane) and $C_2H_2O_2$ (glyoxal); PTR-ToF-MS measurements showed that in all seasons, C_3H_6O is dominant by about 97%. de Gouw and Warneke (2007) indicated that propanal is also negligible and *m/z 59* can be regarded as acetone only. *m/z 60* was assigned to trimethylamine, which is mostly emitted by agricultural activities (Kammer et al., 2019). *m/z 61* is attributed to acetic acid, an agricultural and biogenic compound. *m/z 63* was assigned to dimethylsulfide, emitted by phytoplanktonic activities in the oceans. *m/z 69* was assigned to C_4H_4O: furan and C_5H_8: isoprene and fragments of methylbutenol (MBO), but PTR-ToF-MS measurements showed that MBO is negligible (see discussion of *m/z 87*). Furan is emitted by biomass-burning activities and has highest contributions in autumn and winter (47-67% of m/z 69, Table 2); while in spring and summer, m/z 69 can be almost exclusively attributed to isoprene (94-96%, Table 2), due to its important biogenic source, although it can also be emitted by anthropogenic sources (Borbon et al., 2001; Wagner and Kuttler, 2014; Panopoulou, 2020). *m/z 71* was mainly (by about 85%) attributed to C_4H_6O, the sum of methyl vinyl ketone (MVK), methacrolein (MACR), ISOPOOH, and crotonaldehyde. ISOPOOH are formed from isoprene oxidation under low NO_X conditions (Surratt et al., 2010; Budisulistiorini et al., 2013), and so are expected to be low in a suburban area. In summer, MVK + MACR would be dominant as they are the main isoprene oxidation products, and crotonaldehyde might dominate *m/z 71* in winter, due to its wood burning source (Lipari et al., 1984; Languille et al., 2020). Due to its overall higher level in summer, this m/z will be considered as MVK + MACR. *m/z 73* was mainly attributed to methyl ethyl ketone (MEK) in ambient air (Yuan et al., 2017b). *m/z 75* was identified as $C_3H_6O_2$ (methylacetate, hydroxyacetone, propanoic acid); methylacetate would be a biomass burning compound (Bruns et al., 2017), while hydroxyacetone and propanoic acid are of biogenic origins (Yuan et al., 2017b). It is not possible to separate these compounds because they are isomers, but methylacetate is expected to be the dominant VOC in winter and hydroxyacetone + propanoic acid to be dominant in summer. *m/z 79* was assigned to benzene (C_6H_6). *m/z 81* was assigned to fragments of monoterpenes (mostly) and of PAHs. *m/z 83* was identified as methylfuran (C_5H_6O), that can be found in biomass burning plumes (Bruns et al., 2016), and as a minor oxidation product of isoprene (Kroll et al., 2006; and references therein). This mass was also identified as C_6H_{10}, fragments of hydrocarbons (HC) from gasoline and diesel cars (Gueneron et al., 2015). In winter and autumn, methylfuran is dominant (Table 2) while C_6H_{10} is significant in spring and summer. *m/z 85* was mainly assigned to methylbutenone (C_5H_8O), identified as a biomass burning compound, by (Bruns et al., 2017) and as a biogenic compound by Kroll et al. (2006). *m/z 87* was assigned to $C_4H_6O_2$ (butanedione + methacrylic acid) and $C_5H_{10}O$ (methylbutenol, MBO). Butanedione was found in biomass burning plumes (Bruns et al., 2017), methacrylic acid was identified as an isoprene oxidation product (Williams et al., 2001; Nguyen, 2012) and MBO was shown to be emitted by biogenic sources (Holzinger et al, 2005; Kim et al., 2010). PTR-ToF-MS measurements showed that $C_4H_6O_2$ is dominant (> 80%), thus butanedione would be the main compound in winter and methacrylic acid (MAA) in summer. *m/z 93* was assigned to toluene (C_7H_8), a major traffic compound. *m/z 97* can be attributed to several compounds such as C_2-substituted furans and furaldehydes (Yuan et al.,

2017b), but Bruns et al. (2017) reported this mass as furfural ($C_5H_4O_2$) in biomass-burning influenced regions, and Languille et al. (2020) also defined m/z 97 as furfural in winter at SIRTA. *m/z 99* was identified as $C_5H_6O_2$ (furfuryl alcohol) by Stockwell et al. (2015), and as $C_4H_2O_3$ (furandione) by Bruns et al. (2017), both present in aged biomass burning plumes. In this study, both compounds are present so this mass will be regarded as their sum. *m/z 107* was assigned to C_8H_{10} (C_8-aromatics: xylenes, ethylbenzene) and C_7H_6O (benzaldehyde); C_8-aromatics are dominant by about 80% (Table 2), and thus this mass will be regarded as mainly C_8-aromatics. *m/z 111* was identified as benzenediol by Bruns et al. (2016) as a biomass burning compound. *m/z 121* was assigned to C_9-aromatics (trimethylbenzenes), mainly emitted by traffic. *m/z 137* was assigned to monoterpenes, for which the main source is supposed to be biogenic, although anthropogenic sources, traffic and wood burning, were identified recently (Panopoulou et al., 2020). *m/z 139* was assigned to nopinone, an oxidation product of monoterpenes. *m/z 147* was assigned to dichlorobenzene. *m/z 151* is identified as $C_9H_{10}O_2$, pinonaldehyde, an alpha-pinene ozonolysis product. Pinonaldehyde is measured at m/z 169 and at m/z 151, which corresponds to pinonaldehyde-H_2O.

Section 2: Tables and Figures

Table S1: Instrument parameters throughout the two-year measurement period

Name	Symbol	Value (unit)
Pressure in the drift chamber	P_{drift}	2.2 mbar
Pressure in the detector	P_{detect}	$1.7\text{-}3.3 \cdot 10^{-5}$ mbar
Controlled pressure	$P_{control}$	352-484 mbar
Temperature in the drift chamber	T_{drift}	60 °C
Temperature in the inlet tube	T_{inlet}	60 °C
Voltage in the drift chamber	U_{drift}	600 V
Water flow	F_{H2O}	5–8 $mL \cdot min^{-1}$
Voltage	U_{SO}	90–130 V
Voltage	U_S	80–120 V
Source intensity	I_{hc}	3–6 mA
Voltage in the SEM	U_{SEM}	2000–3500 V
Drift tube length	L	9.2 cm
Collision energy	E/N	134.4 Td

Table S2: Standard canisters used for calibration throughout the two-year measurement period

Start	End	Reference of standard	Composition	VMR
1/18/2020	9/10/2020	R0904, Ionicon Analytik	Methanol, Acetonitrile, Acetaldehyde, Acrolein, Acetone, Isoprene, Crotonaldehyde, 2-Butanone, Benzene, Toluene, o-Xylene, α-pinene, 1,2-Dichlorobenzene	1 ppm
9/10/2020	6/15/2021	L5387, Ionicon Analytik	Methanol, Acetonitrile, Acetone, Isoprene, Benzene, Toluene, Xylenes, Trimethylbenzene, 1,2-Dichlorobenzene	100 ppb
9/1/2021	12/31/2021	D155286, SIAD	Methanol, Acetonitrile, Acetaldehyde, Acrolein, Acetone, MEK, Benzene, Toluene, o-Xylene, α-pinene, 1,2-Dichlorobenzene	1 ppm
5/23/2022	current	NPL	Methanol, Acetonitrile, Acetaldehyde, Acetone, Isoprene, Dimethylsulfide, 3-Buten-2-one, 2-Butanone, Benzene, Toluene, m-Xylene, 1,2,4-Trimethylbenzene, 3-Carene	1 ppm

Table S3: Sensitivity coefficients (ncps/ppb) throughout the 2020-2021 period

Time	SEM voltage (V)	Standard	mz_33 Methanol	mz_42 Acetonitrile	mz_45 Acetaldehyde	mz_57 Propenal	mz_59 Acetone	mz_69 Isoprene
1/15/2020	2975	R0904	10.71	19.52	18.97	17.67	21.22	6.55
1/21/2020	2975	R0904	9.43	18.18	17.63	15.81	19.12	5.72
2/25/2020	2975	R0904	9.63	16.23	15.91	13.83	16.47	4.75
6/11/2020	3100	R0904	11.73	20.13	20.09	18.80	21.90	7.29
7/1/2020	3100	R0904	11.32	20.45	21.37	18.14	22.72	7.24
8/7/2020	3100	R0904	11.97	19.64	19.02	17.97	20.69	6.87
9/10/2020	3050	R0904	11.41	17.01	16.37	14.04	16.86	4.73
10/9/2020	3050	L5387	10.04	17.89			17.15	4.14
11/9/2020	3050	L5387	7.10	17.38			16.91	4.07
12/11/2020	3050	L5387	8.28	16.98			16.96	3.62
1/15/2021	3200	L5387	8.62	21.14			21.32	5.38
1/28/2021	3200	L5387	9.95	21.87			23.14	6.10
2/25/2021	3250	L5387	9.43	22.10			25.41	6.76
4/6/2021	3375	L5387	10.93	24.01			26.82	7.25
4/26/2021	2300	L5387	9.21	18.87			19.19	5.52
5/27/2021	2350	L5387	8.91	19.53			20.04	5.06
8/16/2021	2350	D155286	8.35	14.37	18.72	16.30	21.71	6.46
9/10/2021	2350	D155286	7.87	10.20	12.66	8.58	12.99	3.82
9/20/2021	2350	D155286	7.17	14.19	12.72	8.59	12.12	3.66
10/25/2021	2375	D155286	5.92	10.37	12.05	4.15	10.98	3.31
11/16/2021	2425	D155286	5.43	9.25	11.48	7.99	10.57	2.64
11/16/2021	2425	D155286	5.72	9.50	11.85	8.29	10.71	2.57
12/15/2021	2450	D155286	6.20	10.66	12.25	8.93	11.53	2.84

Time	SEM voltage (V)	Standard	mz_73 MEK	mz_79 Benzene	mz_93 Toluene	mz_107 C8-Aromatics	mz_137 Monoterpenes	mz_147 Dichlorobenzene
1/15/2020	2975	R0904	18.63	8.28	7.95	7.06	1.34	1.65
1/21/2020	2975	R0904	16.39	7.77	7.05	6.03	1.15	1.36
2/25/2020	2975	R0904	13.54	6.12	5.45	4.55	0.84	0.90
6/11/2020	3100	R0904	18.56	9.48	9.20	8.33	1.69	1.94
7/1/2020	3100	R0904	19.75	8.80	8.85	8.01	1.66	1.81
8/7/2020	3100	R0904	17.66	8.37	8.03	7.08	1.39	1.56
9/10/2020	3050	R0904	13.76	5.95	5.43	4.47	0.81	0.94
10/9/2020	3050	L5387		5.31	4.70	3.90		0.84

11/9/2020	3050	L5387		4.99	4.24	3.45		0.80
12/11/2020	3050	L5387		4.52	4.70	3.33		0.68
1/15/2021	3200	L5387		7.68	6.89	6.15		1.52
1/28/2021	3200	L5387		8.23	8.07	6.92		1.75
2/25/2021	3250	L5387		9.72	9.53	8.57		2.08
4/6/2021	3375	L5387		12.23	11.92	10.81		3.26
4/26/2021	2300	L5387		6.81	6.81	4.99		1.42
5/27/2021	2350	L5387		7.28	6.17	4.79		1.32
8/16/2021	2350	D155286	18.65	9.11	8.82	7.76	1.50	1.75
9/10/2021	2350	D155286	10.57	4.35	3.64	2.62	0.44	0.57
9/20/2021	2350	D155286	9.79	4.20	3.31	2.37	0.39	0.45
10/25/2021	2375	D155286	8.63	4.03	3.01	2.10		0.37
11/16/2021	2425	D155286	7.72	3.18	2.45	1.66		0.29
11/16/2021	2425	D155286	7.64	3.37	2.53	1.83		0.29
12/15/2021	2450	D155286	8.57	3.59	2.79	1.97	0.29	0.39

Table S4: Sensitivities (ncps/ppb) obtained for calibrations at various relative humidities

Relative humidity	m/z 33	m/z 42	m/z 45	m/z 59	m/z 69	m/z 71
30 %	8.1	17.0	20.5	22.4	8.6	23.3
60 %	8.1	19.0	18.2	22.1	7.9	21.0
90 %	8.7	19.6	18.8	22.7	8.0	21.9
CV (%)	5	7	6	1	5	5
Relative humidity	m/z 73	m/z 79	m/z 93	m/z 107	m/z 121	m/z 137
30 %	21.9	13.6	14.4	13.6	11.1	4.1
60 %	22.2	13.3	14.4	13.4	10.7	4.1
90 %	22.4	13.2	14.2	13.3	10.8	4.2
CV (%)	1	1	1	1	2	2

CV = coefficient of variation

85

Table S5: Mean and standard deviation values for target bottle measurements

m/z	m/z 33	m/z 42	m/z 45	m/z 46	m/z 57	m/z 59	m/z 60	m/z 61	m/z 69	m/z 71
Mean (ppb)	3.22	0.25	23.68	1.04	1.53	16.58	0.86	0.53	1.82	0.57
Standard deviation	0.72	0.03	2.68	0.57	0.43	0.98	0.16	0.27	0.24	0.17
m/z	m/z 73	m/z 79	m/z 83	m/z 85	m/z 87	m/z 93	m/z 97	m/z 107	m/z 121	
Mean (ppb)	1.38	0.41	0.51	0.31	1.90	0.39	0.39	0.59	0.34	
Standard deviation	0.18	0.05	0.16	0.16	0.32	0.05	0.16	0.10	0.15	

90

Table S6: Descriptive statistics obtained for 2020 and 2021. Values are in ppb.

	Mean 2020	Median 2020	25th percentile 2020	75th percentile 2020	sigma 2020	Mean 2021	Median 2021	25th percentile 2021	75th percentile 2021
Methanol	2.87	2.05	0.96	3.81	2.86	2.87	2.07	1.28	3.46
Acetone	1.06	0.83	0.48	1.31	0.85	0.93	0.70	0.45	1.21
Acetic acid	0.68	0.41	0.21	0.83	0.75	0.58	0.43	0.22	0.80
Acetaldehyde	0.58	0.42	0.26	0.74	0.50	0.61	0.50	0.31	0.80
Ethanol + Formic acid	0.49	0.32	0.16	0.60	0.54	0.49	0.40	0.27	0.63
MEK	0.19	0.14	0.09	0.24	0.17	0.18	0.15	0.09	0.23
Formaldehyde proxy	0.11	0.09	0.04	0.17	0.12	0.09	0.10	0.04	0.16
C3H6O2	0.12	0.07	0.04	0.14	0.12	0.10	0.08	0.05	0.13
MVK+MACR	0.13	0.06	0.03	0.15	0.19	0.06	0.04	0.02	0.07
Butandione + MAA	0.06	0.04	-0.03	0.11	0.12	0.09	0.08	0.02	0.14
Pinonaldehyde	0.06	0.05	0.03	0.10	0.07	0.03	0.01	0.00	0.04
Methylfuran + C6H10	0.06	0.04	0.02	0.07	0.06	0.05	0.04	0.03	0.07
Furfural	0.05	0.03	0.02	0.06	0.06	0.05	0.03	0.02	0.06
Furandione + furfuryl alcohol	0.04	0.03	0.02	0.05	0.04	0.03	0.03	0.02	0.05
Nopinone	0.03	0.03	0.01	0.05	0.04	0.01	0.01	0.00	0.02
Benzenediol	0.03	0.03	0.01	0.05	0.04	0.03	0.02	0.01	0.04
Methylbutenone	0.03	0.02	0.01	0.04	0.03	0.03	0.02	0.01	0.04
Toluene	0.17	0.10	0.06	0.19	0.20	0.18	0.12	0.07	0.22
Benzene	0.13	0.10	0.05	0.16	0.13	0.15	0.13	0.09	0.20
C8_Aromatics	0.14	0.08	0.04	0.16	0.19	0.14	0.09	0.05	0.18
C9_Aromatics	0.08	0.06	0.03	0.11	0.10	0.09	0.06	0.04	0.11
C4H8 + Propenal	0.25	0.18	0.11	0.31	0.24	0.34	0.25	0.14	0.45
Isoprene + Furan	0.24	0.16	0.08	0.29	0.31	0.16	0.12	0.07	0.19
Monoterpenes	0.10	0.07	0.04	0.13	0.15	0.07	0.05	0.03	0.09
Monoterpenes frag	0.05	0.04	0.03	0.06	0.07	0.06	0.04	0.03	0.06
m46	0.53	0.18	0.03	0.57	1.02	0.49	0.20	0.04	0.55
Acetonitrile	0.08	0.07	0.05	0.10	0.04	0.09	0.07	0.05	0.12
Trimethylamine	0.07	0.06	0.04	0.08	0.05	0.06	0.05	0.03	0.08
Allylamine	0.02	0.02	0.01	0.02	0.01	0.02	0.02	0.01	0.02
DMS	0.02	0.02	0.00	0.03	0.03	0.02	0.02	0.01	0.03
Dichlorobenzene	0.03	0.02	0.01	0.05	0.04	0.01	0.01	0.00	0.02
TOTAL	19.11	14.52	8.46	24.09	15.91	17.65	14.49	9.33	23.31

Table S7: Percentage of occurrence of air mass clusters per season

%	DJF	MAM	JJA	SON
Continental	21	37	18	23
Anticyclonic	26	20	24	31
Oceanic 1	45	13	23	19
Oceanic 2	26	21	29	24
North 1	13	35	28	24
North 2	16	40	17	27

Table S8: Mean VOC levels (ppb) per cluster

	Continental	Anticyclonic	Oceanic 1	Oceanic 2	North 1	North 2
Formaldehyde proxy	0.17	0.14	0.03	0.07	0.14	0.09
Methanol	4.57	3.98	1.64	2.02	3.17	1.70
Acetonitrile	0.12	0.10	0.07	0.07	0.10	0.07
Acetaldehyde	1.05	0.76	0.29	0.39	0.74	0.47
mz_46	1.48	0.57	0.05	0.18	0.83	0.50
Ethanol + Formic acid	0.87	0.59	0.24	0.34	0.63	0.38
C_4H_8 + Propenal	0.41	0.36	0.19	0.21	0.39	0.26
Allylamine	0.02	0.02	0.01	0.01	0.02	0.02
Acetone	1.64	1.31	0.62	0.71	1.15	0.63
Trimethylamine	0.10	0.09	0.04	0.05	0.07	0.04
Acetic acid	1.25	0.83	0.25	0.39	0.78	0.49
DMS	0.03	0.03	0.02	0.02	0.02	0.02
Isoprene + Furan	0.28	0.30	0.14	0.14	0.20	0.11
MVK + MACR	0.16	0.14	0.06	0.07	0.10	0.04
MEK	0.32	0.25	0.10	0.12	0.23	0.15
m75 – $C_3H_6O_2$	0.20	0.15	0.05	0.06	0.12	0.08
Benzene	0.23	0.17	0.08	0.10	0.16	0.13
Monoterpenes frag	0.07	0.07	0.04	0.04	0.07	0.04
Methylfuran + C_6H_{10}	0.08	0.08	0.04	0.04	0.07	0.04
Methylbutenone	0.04	0.04	0.02	0.02	0.03	0.02
Butanedione + MAA	0.14	0.12	0.00	0.03	0.11	0.05
Toluene	0.29	0.22	0.08	0.11	0.23	0.13
Furfural	0.07	0.07	0.03	0.03	0.05	0.04
Furandione + furfuryl alcohol	0.06	0.05	0.02	0.03	0.04	0.03

C8-Aromatics	0.24	0.18	0.06	0.09	0.19	0.10
Benzenediol	0.04	0.04	0.02	0.02	0.04	0.03
C9-Aromatics	0.12	0.10	0.05	0.06	0.13	0.07
Monoterpenes	0.11	0.13	0.07	0.06	0.09	0.06
Nopinone	0.03	0.03	0.02	0.01	0.02	0.02
Dichlorobenzene	0.02	0.02	0.01	0.02	0.02	0.02
Pinonaldehyde	0.06	0.06	0.04	0.04	0.04	0.05

Table S9: Correlations of VOCs with external tracers in winter

TRAFFIC WINTERS	R^2	WOOD BURNING WINTERS	R^2	MONOTERPENES WINTERS	R^2
m93xBC_{ff}	0.72	m83xBC_{wb}	0.88	m137xm97	0.23
m107xBC_{ff}	0.80	m85xBC_{wb}	0.83	m137xBC_{ff}	0.30
m121xBC_{ff}	0.77	m87xBC_{wb}	0.53	m137xNO_2	0.23
m93xNO_2	0.65	m97xBC_{wb}	0.75	m137xm93	0.42
m107xNO_2	0.64	m99xBC_{wb}	0.74	m137xm107	0.39
m121xNO_2	0.61	m111xBC_{wb}	0.67	m137xm121	0.37
m93xm107	0.86			m81xm97	0.35
m93xm121	0.85			m81xBC_{ff}	0.43
m107xm121	0.86			m81xNO_2	0.37
				m81xm93	0.59
				m81xm107	0.52
				m81xm121	0.53

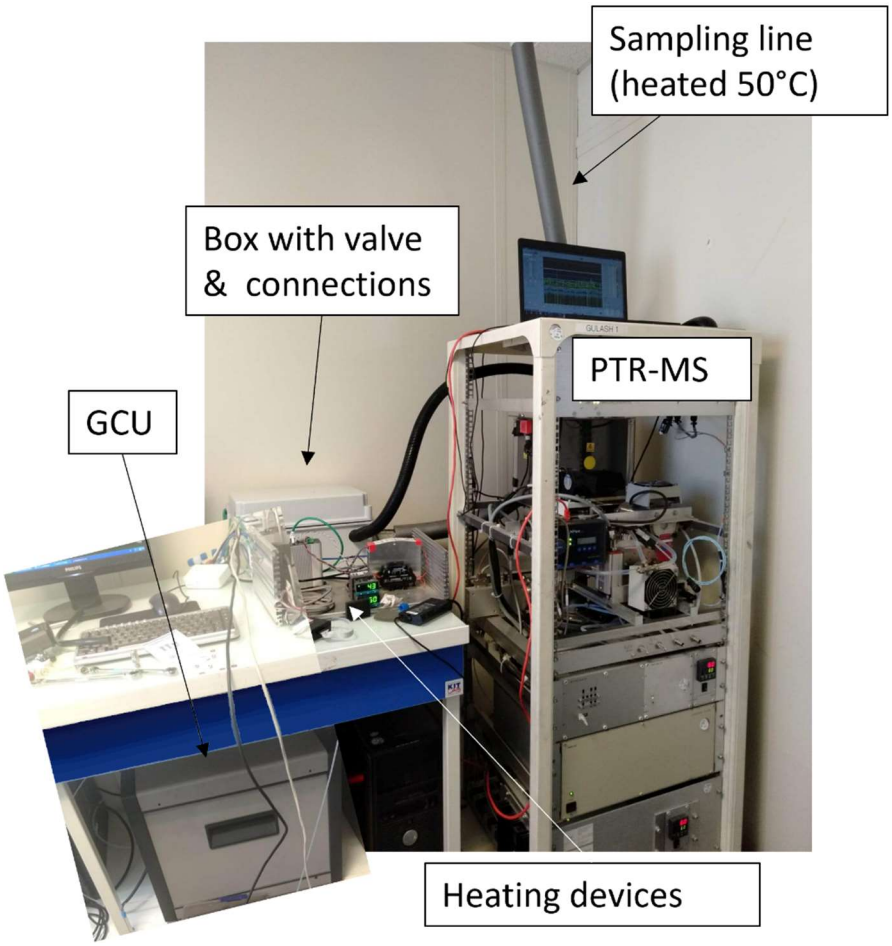

Figure S1: Experimental set-up of the PTR-MS for long-term VOC measurements at SIRTA.

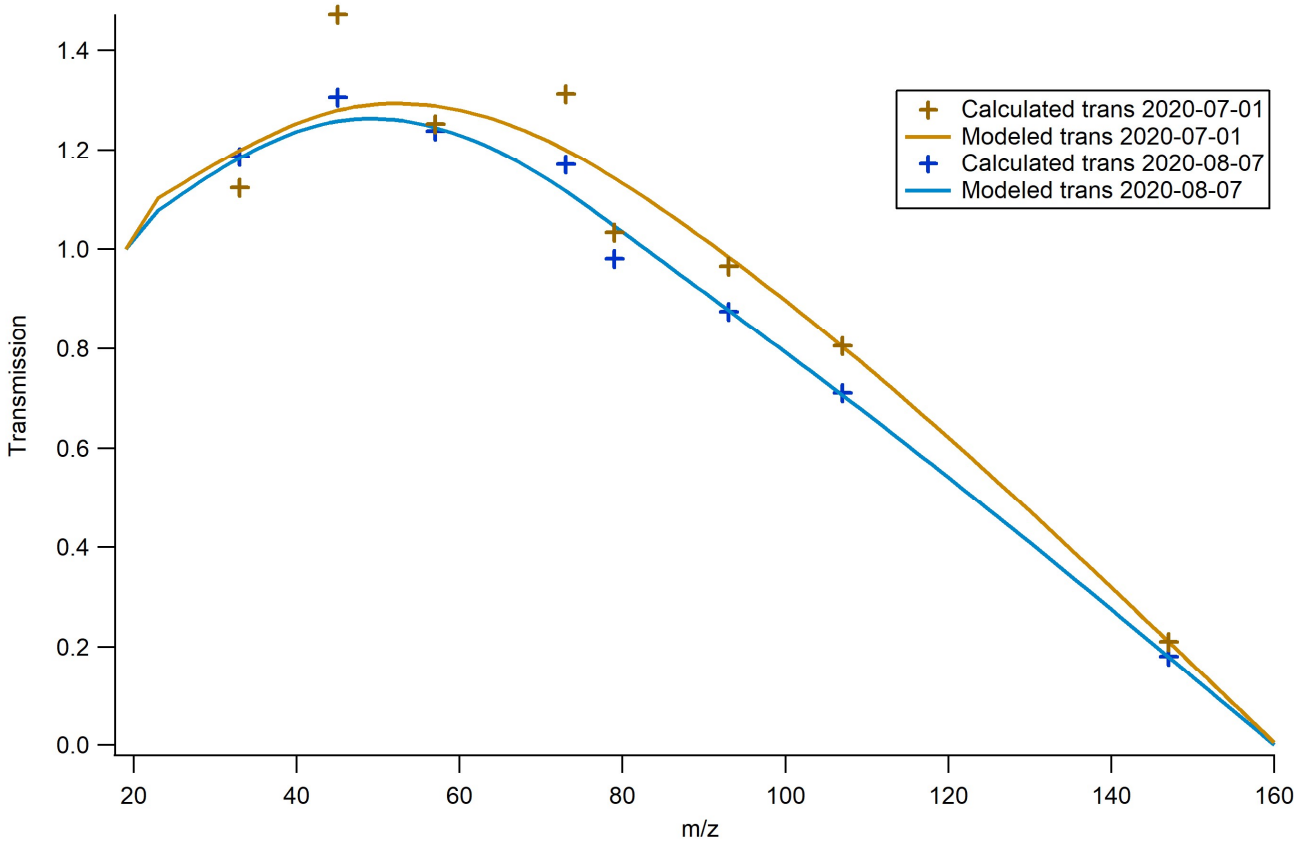

Figure S2: Examples of transmission curves plotted by interpolation of calculated transmissions from the calibrations of 7/1/2020 and 8/7/2020.

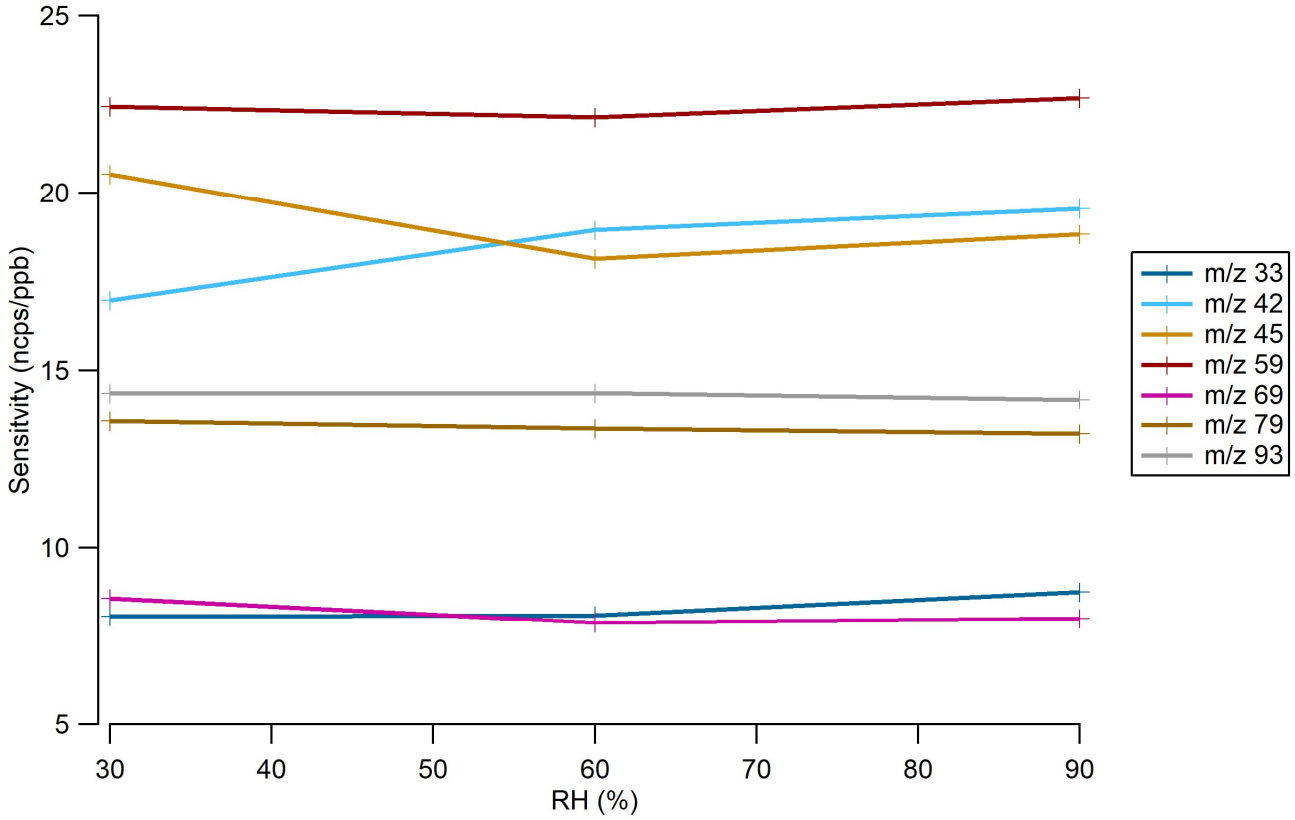

Figure S3: Sensitivities vs RH during the tests performed on August 4th, 2022

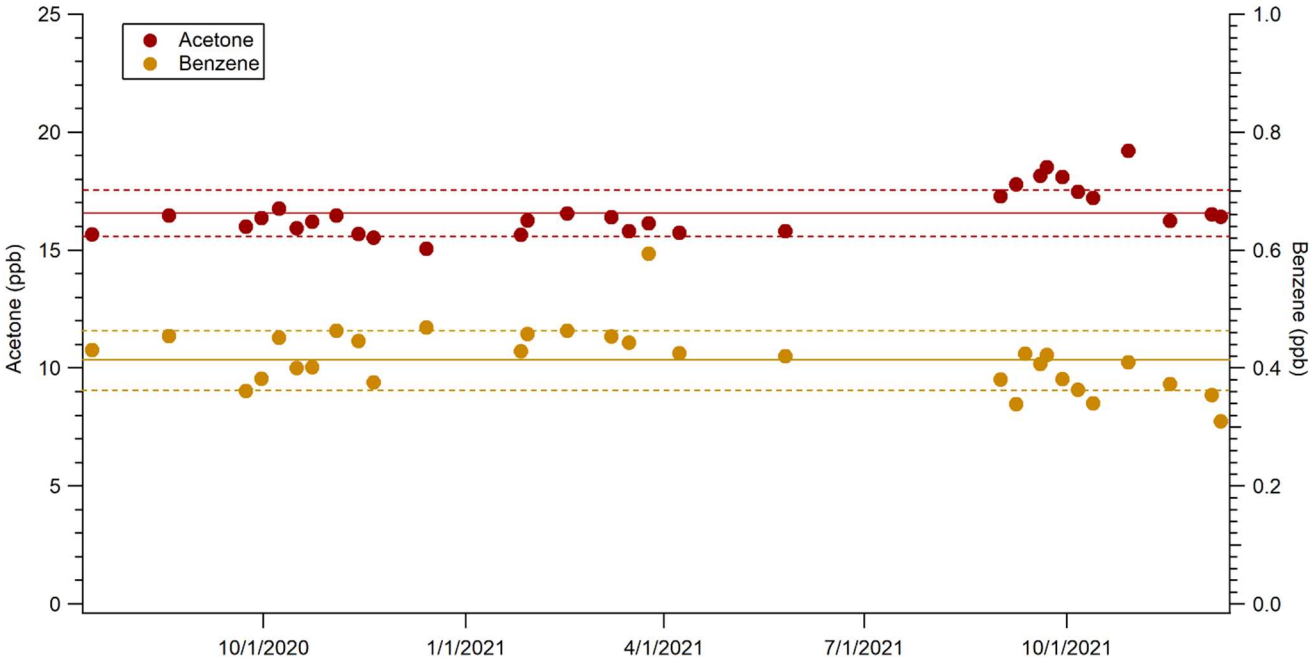

Figure S4: Temporal evolution of acetone and benzene measurements from the target bottle. The lines represent the mean value while the dashed lines represent mean ± standard deviation.

Figure S4 shows the temporal evolution of the measurements of acetone and benzene from the target botle. In 2020 and early 2021, these measurements show small fluctuations but are mainly stable; however, by the end of 2021 the VMR of benzene decreases, due to the lower sensitivity (< 5 ncps/ppb). The PTR-MS underwent an important maintenance early 2022 that solved this issue (benzene sensitivity around 13 ncps/ppb).

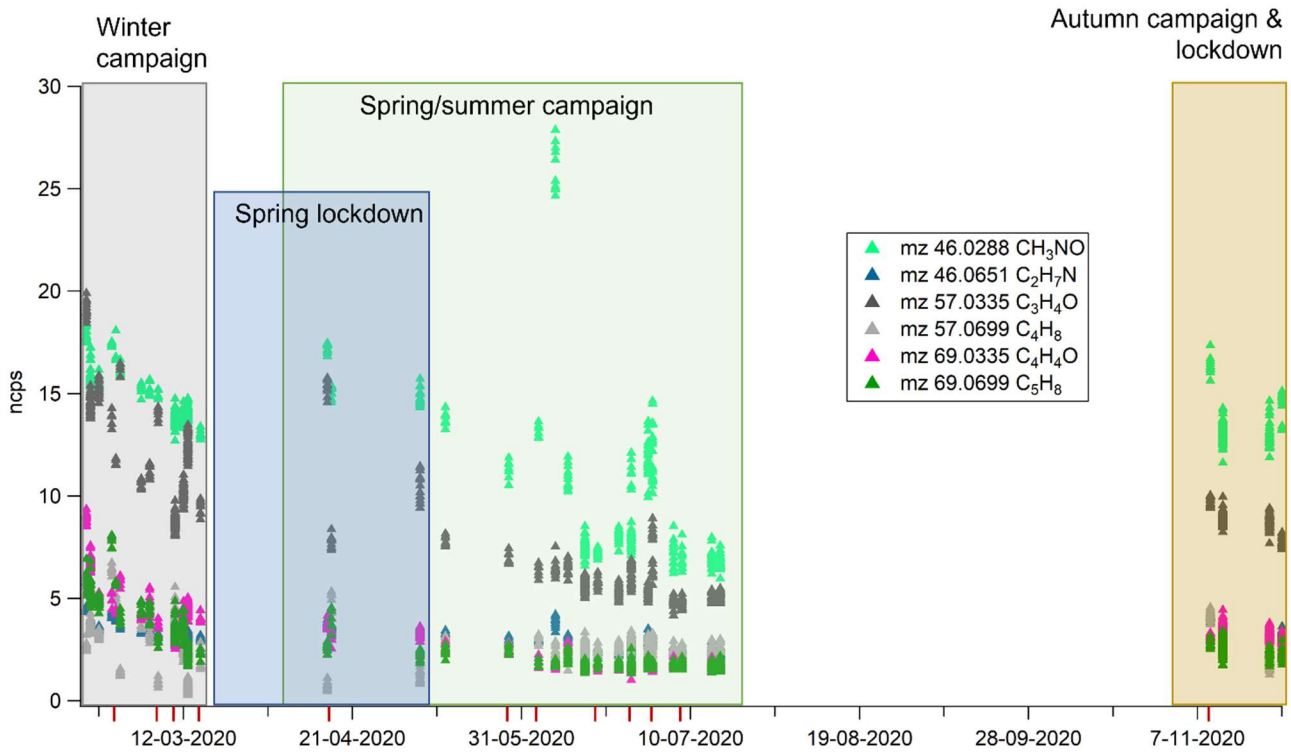

Figure S5: Blanks performed in 2020 for a selection of PTR-ToF-MS m/z. Calibrations are indicated by red sticks.

IONICON

Research & Development
office@ionicon.com

IONICON ANALYTIK GMBH
Eduard-Bodem-Gasse 3
A-6020 Innsbruck
AUSTRIA

Tel: +43 512 214 800
Fax: +43 512 214 800 099
www.ionicon.com

Gas Canister VOC Standard Quality Assurance Certificate

Gas canister serial number: **R2845**

Ionicon guarantees the listed concentrations for a period of 6 months.
Uncertainty is an estimate of a combination of the uncertainties of the original gravimetric preparation and subsequent analysis.

Compound	Volume mixing ratio / ppm	Uncertainty / %
Methanol	0.99	±6
Acetonitrile	0.99	±6
Acetaldehyde	0.95	±5
Ethanol	1.00	±5
Acrolein	1.01	±5
Acetone	0.98	±5
Isoprene	0.95	±5
Crotonaldehyde	1.01	±5
2-Butanone	0.99	±5
Benzene	0.99	±5
Toluene	0.99	±6
o-Xylene	1.02	±6
Chlorobenzene	1.01	±5
a-Pinene	1.01	±5
1,2-Dichlorobenzene	1.02	±5

Gas canisters are filled at a gauge pressure of 2.8 - 3.8 bar and are leak tested for tightness prior to shipping. Should the canister arrive at a pressure lower than the above range, please contact Ionicon immediately; the canister may have developed a leak during transportation and should be returned to Ionicon for refilling.

Jürgen Dunkl
Canister filled by

Signature

10 December 2018
Date

Ionicon Stamp:

IONICON ANALYTIK
Gesellschaft mbH
Eduard-Bodem-Gasse 3
6020 Innsbruck, Austria
Tel.: +43 (0) 512 214 800
Fax: +43 (0) 512 214 800-099
office@ionicon.com
www.IONICON.com

Doc v.4.3; 01.03.2018

Figure S6: Certificate of the canister R2845 used for PTR-ToF-MS calibrations.

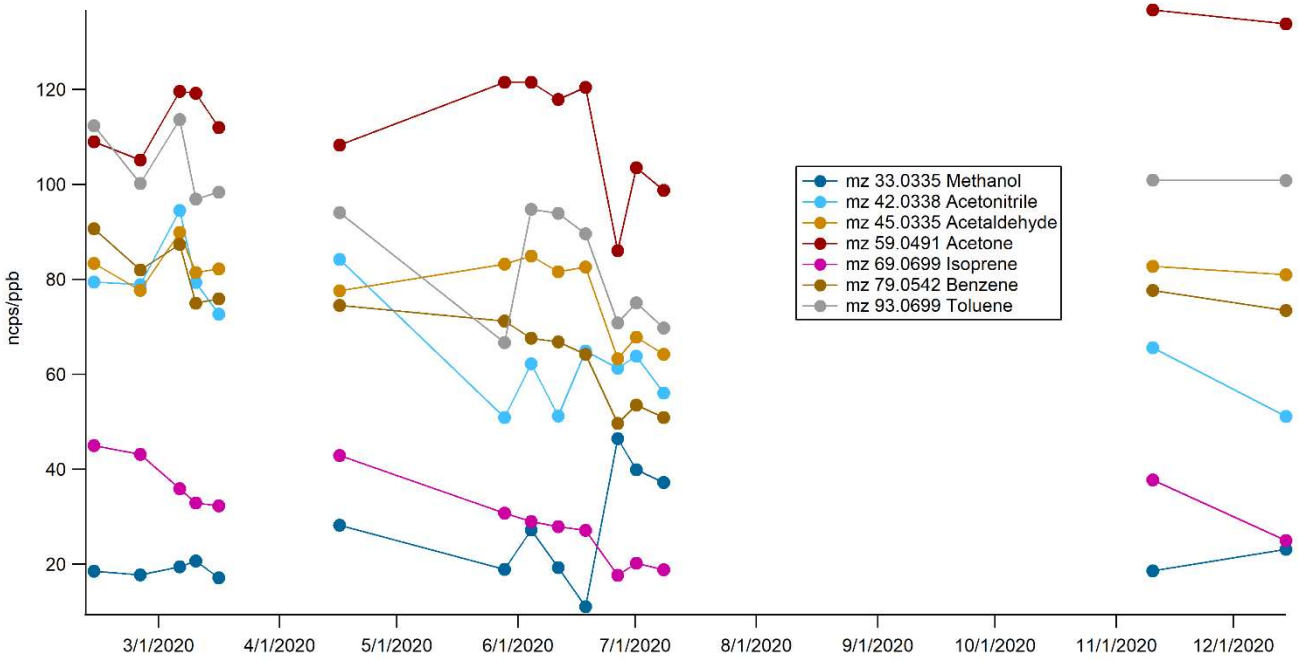

Figure S7: Temporal evolution of measured sensitivities for the PTR-ToF-MS, the different campaigns are separated by the discontinuity of the line.

Figure S7 presents the temporal evolution of the measured sensitivities for the PTR-ToF-MS. The long period with no sensitivity measured between April 16th and May 28th corresponds to the lockdown period. An additional calibration was performed on May 13th, but the sensitivities measured were very low due to little gas left in the canister, so this calibration was not considered.

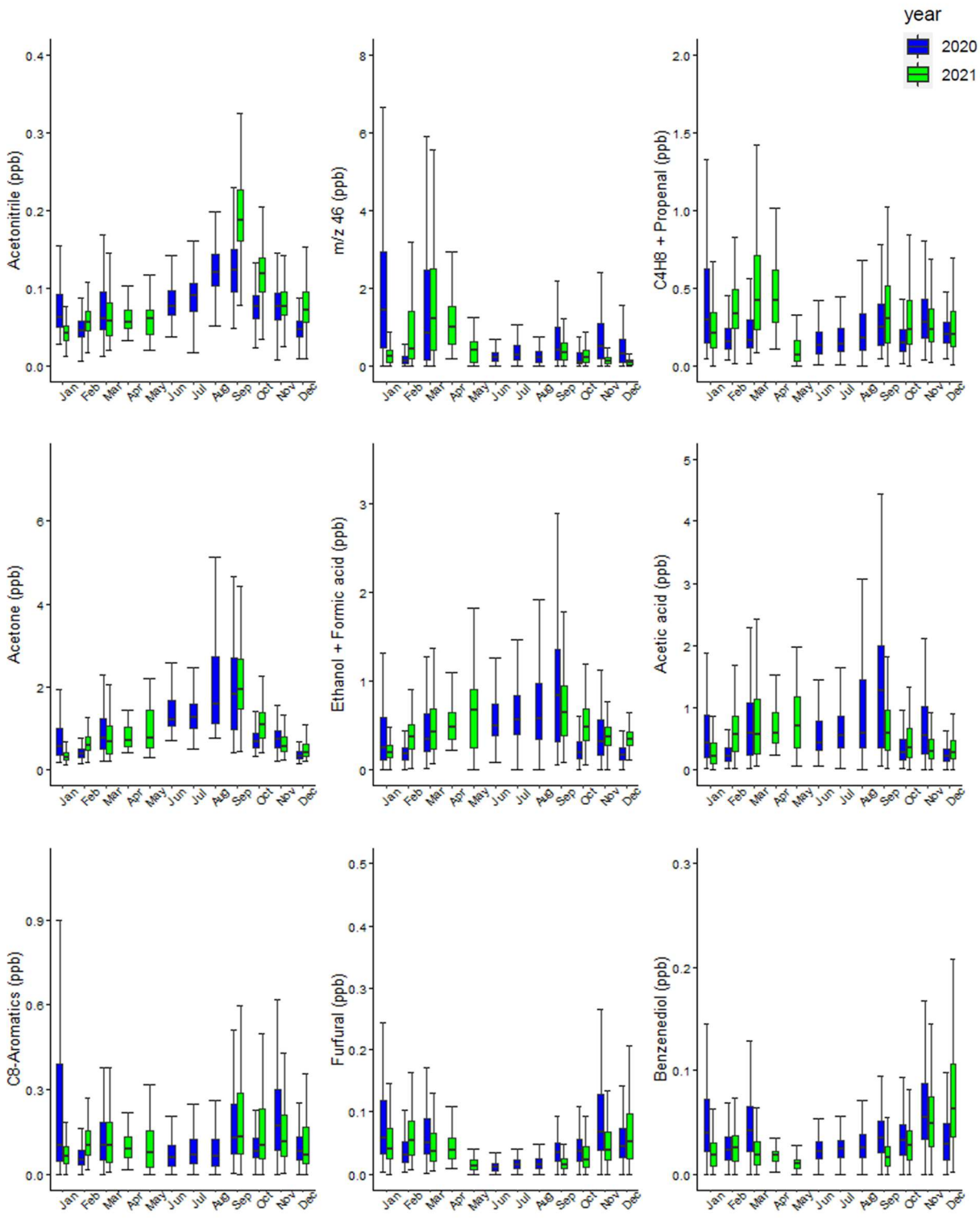
year
2020
2021
Acetonitrile (ppb)
m/z 46 (ppb)
C4H8 + Propenal (ppb)
Acetone (ppb)
Ethanol + Formic acid (ppb)
Acetic acid (ppb)
C8-Aromatics (ppb)
Furfural (ppb)
Benzenediol (ppb)
Jan
Feb
Mar
Apr
May
Jun
Jul
Aug
Sep
Oct
Nov
Dec

Figure S8: Monthly distribution of Furfural (m/z 97) for 2020 (blue) and 2021 (green). Boxes represent 25th and 75th percentiles, the line is the median. Whiskers represent 5th and 95th percentiles

Figure S9: Map for the location of the Airparif station with respect to SIRTA

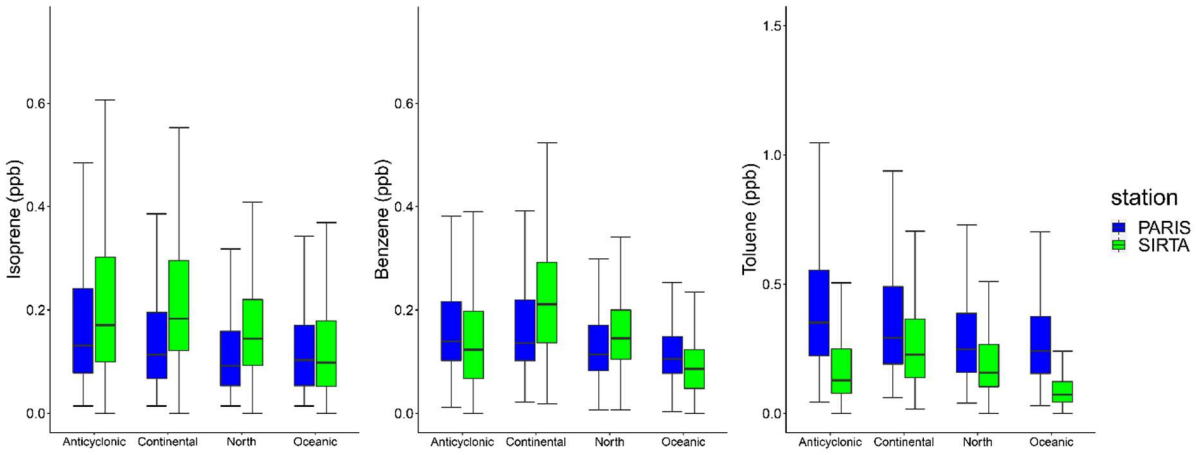

155 **Figure S10: Statistic distribution of measurements at SIRTA and Paris centre of isoprene, benzene, and toluene for the different air mass clusters. The line in the middle of the box is the median, lower and upper hinges are 25th and 75th percentiles, respectively. Lower and upper whiskers are lower hinge - 1.5 IQR and upper hinge + 1.5 IQR, respectively.**

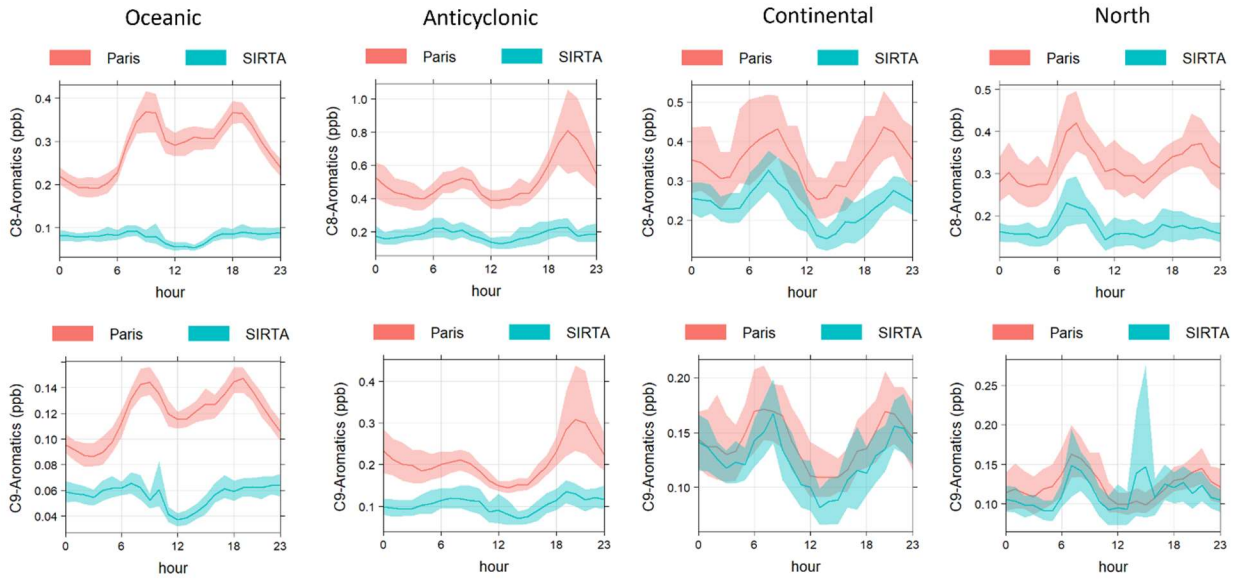

Figure S11: Diel cycles of benzene, C8- and C9-aromatics at SIRTA and at Paris centre for oceanic, North, anticyclonic and 160 **continental air masses.**

References

Aoki, N., Inomata, S., and Tanimoto, H.: Detection of C1–C5 alkyl nitrates by proton transfer reaction time-of-flight mass spectrometry, International Journal of Mass Spectrometry, 263, 12–21, https://doi.org/10.1016/j.ijms.2006.11.018, 2007.

Borbon, A., Fontaine, H., Veillerot, M., Locoge, N., Galloo, J. C., and Guillermo, R.: An investigation into the traffic-related fraction of isoprene at an urban location, Atmospheric Environment, 35, 3749–3760, https://doi.org/10.1016/S1352-2310(01)00170-4, 2001.

Bruns, E. A., El Haddad, I., Slowik, J. G., Kilic, D., Klein, F., Baltensperger, U., and Prévôt, A. S. H.: Identification of significant precursor gases of secondary organic aerosols from residential wood combustion, Sci Rep, 6, 27881, https://doi.org/10.1038/srep27881, 2016.

Bruns, E. A., Slowik, J. G., El Haddad, I., Kilic, D., Klein, F., Dommen, J., Temime-Roussel, B., Marchand, N., Baltensperger, U., and Prévôt, A. S. H.: Characterization of gas-phase organics using proton transfer reaction time-of-flight mass spectrometry: fresh and aged residential wood combustion emissions, Atmos. Chem. Phys., 17, 705–720, https://doi.org/10.5194/acp-17-705-2017, 2017.

Budisulistiorini, S. H., Canagaratna, M. R., Croteau, P. L., Marth, W. J., Baumann, K., Edgerton, E. S., Shaw, S. L., Knipping, E. M., Worsnop, D. R., Jayne, J. T., Gold, A., and Surratt, J. D.: Real-Time Continuous Characterization of Secondary Organic Aerosol Derived from Isoprene Epoxydiols in Downtown Atlanta, Georgia, Using the Aerodyne Aerosol Chemical Speciation Monitor, Environ. Sci. Technol., 47, 5686–5694, https://doi.org/10.1021/es400023n, 2013.

Duncianu, M., David, M., Kartigueyane, S., Cirtog, M., Doussin, J.-F., and Picquet-Varrault, B.: Measurement of alkyl and multifunctional organic nitrates by proton-transfer-reaction mass spectrometry, Atmos. Meas. Tech., 10, 1445–1463, https://doi.org/10.5194/amt-10-1445-2017, 2017.

de Gouw, J. and Warneke, C.: Measurements of volatile organic compounds in the earth's atmosphere using proton-transfer-reaction mass spectrometry, Mass Spectrom. Rev., 26, 223–257, https://doi.org/10.1002/mas.20119, 2007.

Gueneron, M., Erickson, M. H., VanderSchelden, G. S., and Jobson, B. T.: PTR-MS fragmentation patterns of gasoline hydrocarbons, International Journal of Mass Spectrometry, 379, 97–109, https://doi.org/10.1016/j.ijms.2015.01.001, 2015.

Holzinger, R., Lee, A., Paw U, K T, and Goldstein, A. H.: Observations of oxidation products above a forest imply biogenic emissions of very reactive compounds, Atmos. Chem. Phys., 9, 2005.

Holzinger, R.: PTRwid: A new widget tool for processing PTR-TOF-MS data, Atmos. Meas. Tech., 8, 3903–3922, https://doi.org/10.5194/amt-8-3903-2015, 2015.

Kammer, J., Décuq, C., Baisnée, D., Ciuraru, R., Lafouge, F., Buysse, P., Bsaibes, S., Henderson, B., Cristescu, S. M., Benabdallah, R., Chandra, V., Durand, B., Fanucci, O., Petit, J.-E., Truong, F., Bonnaire, N., Sarda-Estève, R., Gros, V., and Loubet, B.: Characterization of particulate and gaseous pollutants from a French dairy and sheep farm, Science of The Total Environment, 135598, https://doi.org/10.1016/j.scitotenv.2019.135598, 2019.

Kim, S., Karl, T., Guenther, A., Tyndall, G., Orlando, J., Harley, P., Rasmussen, R., and Apel, E.: Emissions and ambient distributions of Biogenic Volatile Organic Compounds (BVOC) in a ponderosa pine ecosystem: interpretation of PTR-MS mass spectra, Atmos. Chem. Phys., 13, 2010.

Knighton, W. B., Herndon, S. C., Shorter, J. H., Miake-Lye, R. C., Zahniser, M. S., Akiyama, K., Shimono, A., Kitasaka, K., Shimajiri, H., and Sugihara, K.: Laboratory Evaluation of an Aldehyde Scrubber System Specifically for the Detection of Acrolein, Journal of the Air & Waste Management Association, 57, 1370–1378, https://doi.org/10.3155/1047-3289.57.11.1370, 2007.

Kroll, J. H., Ng, N. L., Murphy, S. M., Flagan, R. C., and Seinfeld, J. H.: Secondary Organic Aerosol Formation from Isoprene Photooxidation, Environ. Sci. Technol., 40, 1869–1877, https://doi.org/10.1021/es0524301, 2006.

Languille, B., Gros, V., Petit, J.-E., Honoré, C., Baudic, A., Perrussel, O., Foret, G., Michoud, V., Truong, F., Bonnaire, N., Sarda-Estève, R., Delmotte, M., Feron, A., Maisonneuve, F., Gaimoz, C., Formenti, P., Kotthaus, S., Haeffelin, M., and Favez, O.: Wood burning: A major source of Volatile Organic Compounds during wintertime in the Paris region, Science of The Total Environment, 711, 135055, https://doi.org/10.1016/j.scitotenv.2019.135055, 2020.

Lindinger, W., Jordan, A., and Hansel, A: Proton-transfer-reaction mass spectrometry (PTR–MS): on-line monitoring of volatile organic compounds at pptv levels, Chem. Soc. Rev., 27, 347, https://doi.org/10.1039/a827347z, 1998.

Lipari, Frank., Dasch, J. M., and Scruggs, W. F.: Aldehyde emissions from wood-burning fireplaces, Environ. Sci. Technol., 18, 326–330, https://doi.org/10.1021/es00123a007, 1984.

Panopoulou, A.: Yearlong measurements of monoterpenes and isoprene in a Mediterranean city (Athens): Natural vs anthropogenic origin, Atmospheric Environment, 12, 2020.

Panopoulou, A., Liakakou, E., Sauvage, S., Gros, V., Locoge, N., Stavroulas, I., Bonsang, B., Gerasopoulos, E., and Mihalopoulos, N.: Yearlong measurements of monoterpenes and isoprene in a Mediterranean city (Athens): Natural vs anthropogenic origin, Atmospheric Environment, 243, 117803, https://doi.org/10.1016/j.atmosenv.2020.117803, 2020.

Španěl, P., Wang, T., and Smith, D.: A selected ion flow tube, SIFT, study of the reactions of H3O+, NO+ and O2+ ions with a series of diols, International Journal of Mass Spectrometry, 218, 227–236, https://doi.org/10.1016/S1387-3806(02)00724-8, 2002.

Stockwell, C. E., Veres, P. R., Williams, J., and Yokelson, R. J.: Characterization of biomass burning emissions from cooking fires, peat, crop residue, and other fuels with high-resolution proton-transfer-reaction time-of-flight mass spectrometry, Atmos. Chem. Phys., 15, 845–865, https://doi.org/10.5194/acp-15-845-2015, 2015.

Surratt, J. D., Chan, A. W. H., Eddingsaas, N. C., Chan, M., Loza, C. L., Kwan, A. J., Hersey, S. P., Flagan, R. C., Wennberg, P. O., and Seinfeld, J. H.: Reactive intermediates revealed in secondary organic aerosol formation from isoprene, Proceedings of the National Academy of Sciences, 107, 6640–6645, https://doi.org/10.1073/pnas.0911114107, 2010.

Taipale, R., Ruuskanen, T. M., Rinne, J., Kajos, M. K., Hakola, H., Pohja, T., and Kulmala, M.: Technical Note: Quantitative long-term measurements of VOC concentrations by PTR-MS – measurement, calibration, and volume mixing ratio calculation methods, Atmos. Chem. Phys., 18, 2008.

Wagner, P. and Kuttler, W.: Biogenic and anthropogenic isoprene in the near-surface urban atmosphere — A case study in Essen, Germany, Science of The Total Environment, 475, 104–115, https://doi.org/10.1016/j.scitotenv.2013.12.026, 2014.

Williams, J., Pöschl, U., Crutzen, P. J., Hansel, A., Holzinger, R., Warneke, C., Lindinger, W., and Lelieveld, J.: An Atmospheric Chemistry Interpretation of Mass Scans Obtained from a Proton Transfer Mass Spectrometer Flown over the Tropical Rainforest of Surinam, 34, n.d.

Yuan, B., Coggon, M. M., Koss, A. R., Warneke, C., Eilerman, S., Peischl, J., Aikin, K. C., Ryerson, T. B., and de Gouw, J. A.: Emissions of volatile organic compounds (VOCs) from concentrated animal feeding operations (CAFOs): chemical compositions and separation of sources, Atmos. Chem. Phys., 17, 4945–4956, https://doi.org/10.5194/acp-17-4945-2017, 2017a.

Yuan, B., Koss, A. R., Warneke, C., Coggon, M., and Sekimoto, K.: Proton-Transfer-Reaction Mass Spectrometry: Applications in Atmospheric Sciences, Chem. Rev., 43, 2017b.

Zhao, J. and Zhang, R.: Proton transfer reaction rate constants between hydronium ion (H3O+) and volatile organic compounds, Atmospheric Environment, 38, 2177–2185, https://doi.org/10.1016/j.atmosenv.2004.01.019, 2004.